

Laser interferometric measuring system for positioning in nanometrology

JOSEF LAZAR, ONDŘEJ ČÍP, MARTIN ČÍŽEK, JAN HRABINA, AND MOJMÍR ŠERÝ

Department of Coherence Optics
Institute of Scientific Instruments, Academy of Sciences of the Czech Republic
Královopolská 147, 612 64 Brno
CZECH REPUBLIC

PETR KLAPETEK
Department of Nanometrology
Czech Metrology Institute
Okružní 31, 638 00 Brno
CZECH REPUBLIC

joe@isibrno.cz <http://www.isibrno.cz>

Abstract: - In this contribution we present a development of a system for dimensional nanometrology based on scanning probe microscopy techniques (primarily atomic force microscopy, AFM) for detection of sample profile combined with interferometer controlled positioning. The key goal for introduction of interferometer measurement is not only improvement of resolution but the direct traceability to the primary etalon of length. Interferometry compared to a host of other optical length measuring techniques [1,2,3...] represents the most precise measuring technique available. The system is being developed to operate at and in cooperation with the Czech metrology institute for calibration purposes and nanometrology.

Keywords- Nanometrology, Interferometry, Traceability, Local probe microscopy, Nanopositioning.

1. Introduction

Dimensional metrology dealing with objects in the micro- and nanoworld relies predominantly on AFM (Atomic Force Microscope) and related local probe microscopy techniques where the object topology, dimensions and other properties are examined by scanning the sample. Positioning of the probe in AFM microscopes through piezoelectric (PZT) transducers offers sub-nm resolution but small range over several tens of micrometers. More, PZT transducers suffer errors of repeatability, non-linearity and hysteresis. Metrological AFM can be calibrated using etalon gratings or samples of height staircase type in the scale of hundreds or thousands of nanometers.

The problem of traceability [4] is a complex one where a system independent on an etalon samples should be linked directly to the primary etalon of length. This means employment of laser interferometry techniques for measurement of the probe position and taking care for all other sources of error starting with the uncertainty of the laser optical frequency [5]. Systems designed to follow

this demand represent a setup mostly consisting of an AFM head, positioning stage and displacement measuring arrangement where a multiaxis laser interferometers dominate [6,7,8] but other approaches based on optical methods may represent suitable solution [9]. Measurement of the sample position in three orthogonal axes is sufficient when the guides of the stage can ensure negligible angle errors. Full control of the stage position should engage evaluation of tilting of the stage where non-contact optical methods a preferred [10]. A more complex interferometric measuring system needs also a complex approach to all sources of errors caused by angle deviations from orthogonality of the measuring beams, angle errors of reflecting surfaces, etc. [11]. Interferometric measuring techniques in dimensional metrology are well established and represent a link between the fundamental etalon of length and mechanical measuring systems. Significant effort has been invested into improvement of their performance in the nanoscale through linearization of the fringe interpolation [12].

Transforming the local probe microscope from an imaging tool into a measuring system for metrological purposes means replacement of the often small scale positioning of the probe with an external stage moving

the sample and interferometric monitoring or even control.

Laser interferometry seems to be a solution not only due to its direct traceability to the fundamental etalon of length but also the incremental interferometer in its fringe counting mode gives an excellent dynamic range limited only by the fluctuations of the refractive index of air and offers nanometer or even subnanometer resolution over large range. We concentrated onto a small range flexure three-axis nanopositioning stage equipped with closed-loop motion control with capacitive sensors embedded in a frame with six-axes interferometric system supplied from a stabilized single-frequency frequency doubled 532 nm Nd:YAG laser.

2. Stage Design

In the design presented here we concentrated on a commercial positioning stage with $200 \times 200 \times 10 \mu\text{m}$ travel and its enclosure into a frame containing interferometric displacement monitoring system. Full control of the stage and evaluation of all its positioning errors needs six-axis measurement. In our arrangement we equipped the stage with a top plate – a sample holder and a set of flat mirrors. It overlaps the stage and makes possible the measurement of the vertical displacement around the stage by three interferometers pointing upwards. Together with the mount of the local probe microscope the side view is in Figure 1. Thus the vertical position in the z-axis together with pitch and roll angles can be evaluated.

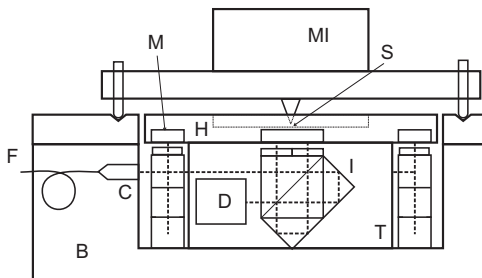


Figure 1: Side view of the stage with vertical interferometers, B: baseplate, MI: microscope, S: sample, F: fiber light delivery, C: collimator, H: sample holder, T: stage, I: interferometer, D: homodyne detection unit, M: mirror

Horizontal measurement of x- and y- axes is ensured by three interferometers which allow also evaluation of the yaw. Interferometers are with flat-mirror reflector and

a fixed corner-cube reflector in both reference arm and measuring arm. Double-pass arrangement enhances resolution in simple fringe-counting regime to $\lambda/4$ (Figure 2).

The resolution of the interferometric detection and data processing system here is 10 bit with 1 LSB being the $1/1024$ of one cycle of the interferometric signal. Together with the double beam pass it results in $\lambda/4096$ which means for the 532 nm wavelength resolution 130 pm

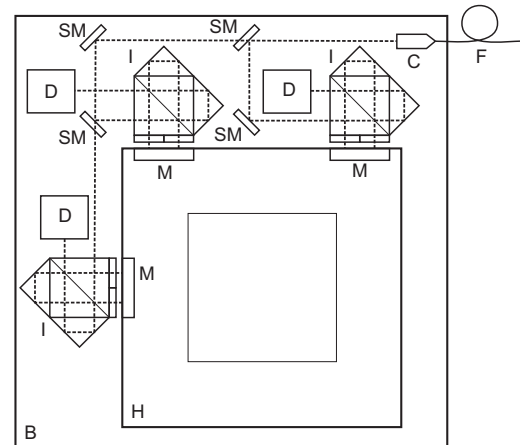


Figure 2: Top view of the interferometric configuration with measurement in the x- and y-axes, SM: beam steering mirror, others see Figure 1.

Compensation for the fluctuations of the refractive index in interferometric systems is traditionally ensured through the evaluation of the Edlen formula and under laboratory conditions results in relative uncertainty between 10^{-6} and 10^{-7} . Here when due to small dead length (0.1 mm) and travel range the maximum length of the measuring arm is 0.3 mm. The influence of the refractive index of air may prove significant only at the 0.3 nm level.

The small range of positioning ranging within $200 \mu\text{m}$ in the horizontal plane and only $10 \mu\text{m}$ in the vertical axis enhances the importance of the linearity of the scale. Linearity of the fringe division is further improved by software linearization algorithm embedded directly into the signal processing of the interferometer signal [13,14]. With the shorter wavelength of the green laser (compared with the traditional 633 nm red He-Ne laser of commercial interferometers) another small resolution improvement was achieved.

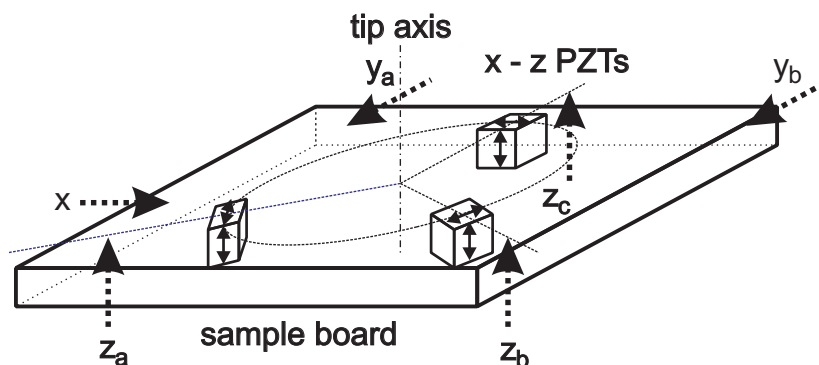


Figure 3: Arrangement of the additional three PZT transducers compensating for the angle errors. x , y_a , y_b , z_a , z_b , z_c : orientation of interferometers.

The chance to evaluate the angle deviations offers a good opportunity to compensate for them. Angle deviations of the reflective mirrors in a plane-mirror interferometric design results in angle-induced errors due to difference between the returning beam path and the axis of motion. We introduced a set of three piezoelectric transducers (PZT) each with two directions of motion: vertical and sheering horizontal (Figure 3). Their arrangement around the centre of the table with the horizontal axes of motion being oriented tangentially gives a chance to control all the angle errors.

In the first pilot design we looked for the level of angle deviations and decided for PZT transducers with 3 μm travel in the vertical axis and 5 μm in the horizontal. The horizontal motion of all three transducers oriented tangentially rotates the stage with respect to the vertical axis.

3. Laser Source

Traditional dimensional interferometry has been a domain of stabilized He-Ne lasers operating at the 633 nm wavelength. Their single- or two-frequency operation, narrow linewidth, modest output power and relative simplicity were among their advantages. Stabilization of optical frequency was based here on various detection techniques of the Doppler-broadened spectral profile of the active line in Ne. With the fluctuations of the refractive index of air influencing the interferometric measurements in the 10^{-6} , in the best case in the 10^{-7} order even with precise compensation through the Edlen formula the stability achieved proved to be sufficient.

Output power of a single-frequency He-Ne laser in the range of 1 mW is enough to supply an interferometric system with a single-axis measurement. Splitting of the laser beam into several discrete interferometers usually needs to rise gain in the detection chain and thus to worsen the noise performance of the system.

In our case we intended to assemble a displacement measurement arrangement which would monitor the nano-positioning table in all six axes of freedom. Feeding six discrete interferometers would be a difficult task for a low-power He-Ne laser especially when it seems suitable to apply a fiber optic light delivery system. A free-space to fiber coupler and a splitter causes considerable losses. In the first design we arranged the laser and light delivery scheme with two fibre optic branches and a stabilization scheme with iodine cell according to fig. 4.

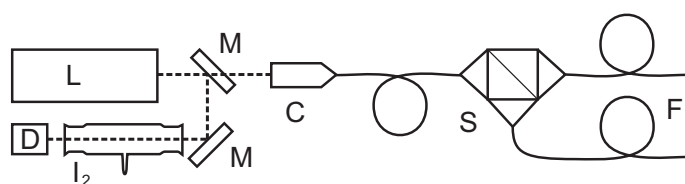


Figure 4: First setup of laser stabilization and two-branch fibre optic light delivery, L: laser, M: mirrors, D: photodetector, F: polarization maintaining fiber, C: collimator, S: non-polarizing beamsplitter, I_2 : iodine cell.

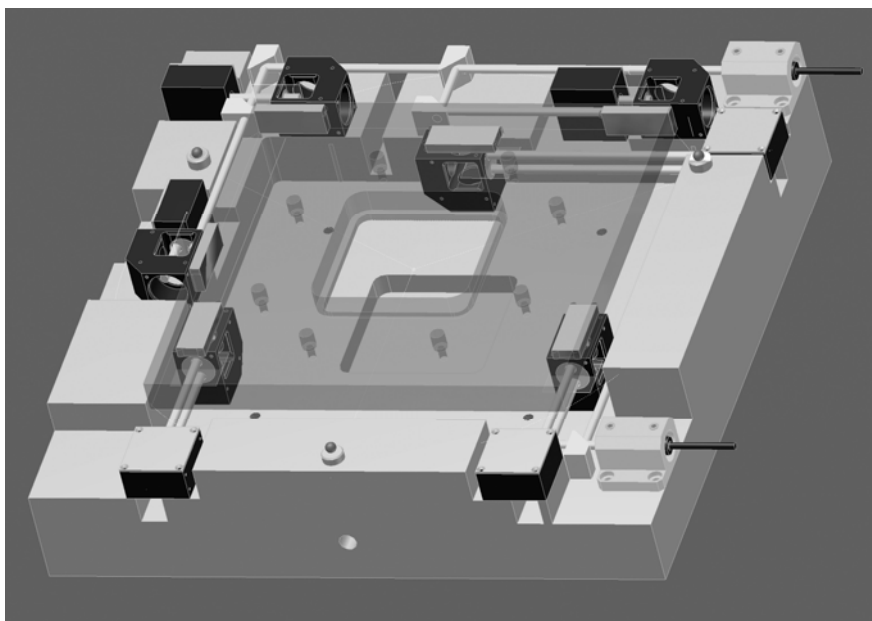


Figure 5: Mechanical design of the interferometer frame for embedding of the nanopositioning stage. The stage itself is omitted here, the transparent upper board serves as a mirror holder and sample holder.

We decided for a more powerful and proven frequency doubled Nd:YAG laser operating at the 532 nm wavelength, a laser with high-efficiency intracavity doubling designed for primary laser optical frequency etalons. Interferometric detection systems used in our designs are based on DC, homodyne detection principle and need a single-frequency laser operation. This made our choice easier while generation of two closely spaced stable optical frequencies would not be easy with a solid-state laser.

Our Nd:YAG laser features low amplitude noise and output power on the 100 mW level. The short-term intrinsic optical frequency stability of the free running laser satisfies well the requirements of interferometry in the presence of air where the fluctuations of index of refraction are the main limiting factor. This is ensured by thermal stabilization of the active crystal and the laser cavity.

The laser is stabilized through a linear spectroscopy in molecular iodine by locking to a Doppler broadened absorption of a transition which is in coincidence with the laser tuning range. This follows the recommendations of CIPM [5] and ensures the traceability to fundamental etalon. Stabilization to the Doppler broadened spectral profile is able to deliver stabilities in the range of 10^{-8} which is here at least one order better than the influence of variations of the refractive index of air.

4. Light Delivery

The first configuration presented here with two-branch fiber optic delivery is in Fig. 5. Interferometers are arranged in two levels with steering of the laser beams to discrete interferometric units via semireflecting mirrors within each level. On the right of the stage mount there are collimators for each level. Simplicity of the fiber optic assembly with cheap components (fiber optic splitter) needed a complex set of precisely adjustable mirrors. This proved to be a great obstacle to elimination of primary angle errors, cosine and Abbe errors in all axis of measurement. Independent and precision angle steering of each of the interferometric unit proved to be necessary.

The the first configuration the laser radiation was delivered to the interferometers via a single-mode polarization maintaining fiber and split into the measuring axes by a 50/50% non-polarizing splitter incorporated into the fiber-optic assembly. The two arms of the fiber-optic delivery supply three interferometers each. First are the three interferometers measuring in the z-axis are arranged in one plane and the other are the x and double y measuring interferometers in other plane.

The key problem of a complex fiber optic assembly for independent light delivery proved to be the polarization maintaining fiber. A set of tests was performed to find a suitable fiber and a splitter with

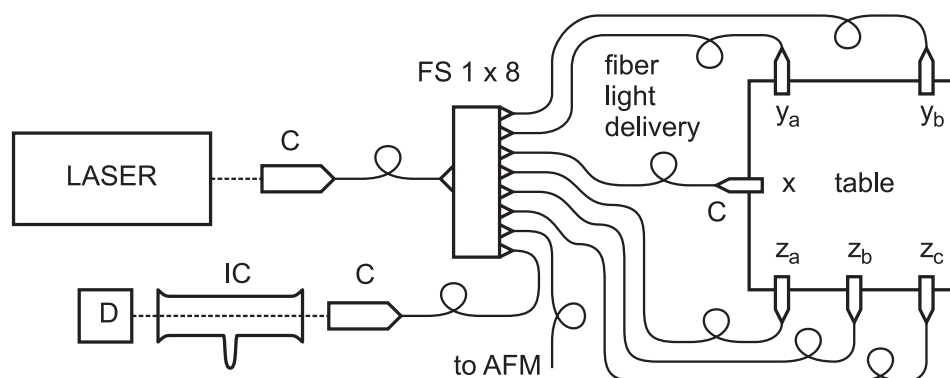


Figure 6: Laser source with stabilization of frequency through linear spectroscopy in iodine and light delivery arrangement. LASER: Frequency doubled Nd:YAG laser, C: fiber collimators, FS: fiber polarization maintaining splitter, D: photodetector, IC: iodine cell.

acceptably low sensitivity to stress and thermal effects. We applied a polarization maintaining splitter with one input and 8 outputs where the light delivery to the iodine cell was via a fiber as well. The final 8th output was reserved for a 7th interferometer which is intended to monitor the vertical positioning of the AFM tip. Configuration of the full independent fiber optic light delivery system is in Fig. 6.

The arrangement of the modified frame with interferometers supplied from a discrete fiber each is in Fig. 7. The three vertical interferometers are hidden below the sample table and a board on the left represents the fiber splitter. Each output collimator is housed in a positioner with four degrees of freedom and fine adjusting screws.

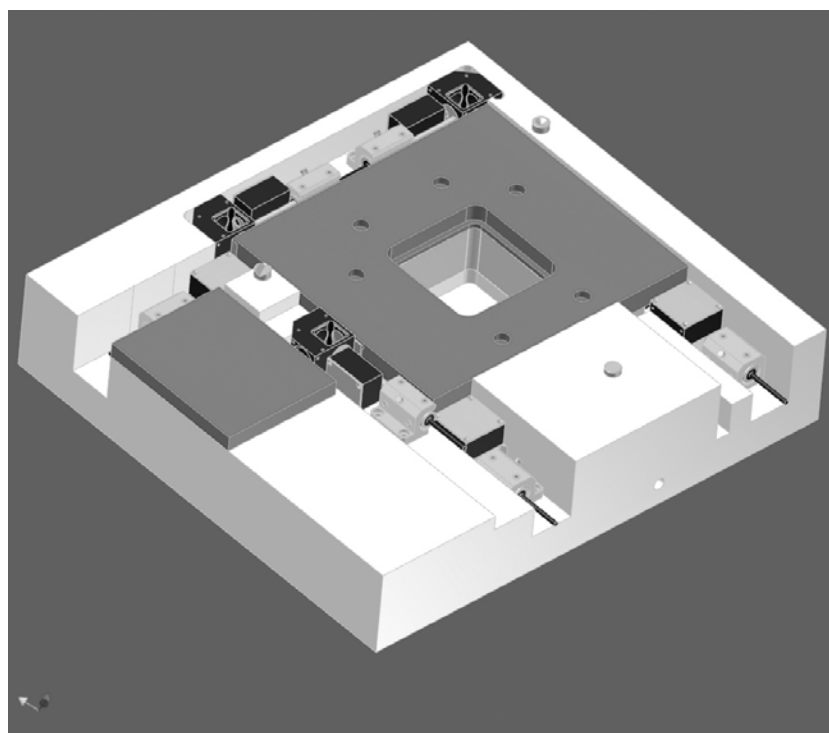


Figure 7: New mechanical design of the interferometer frame with independent fiber light delivery and 1/8 fiber optic polarization maintaining splitter.

5. Evaluation and Testing

The positioning performance of the “free-running” stage (without feedback control of angle via additional PZTs) was tested through evaluation of the angle errors. The calculated angle deviations of the stage during full-range travel are presented in Figure 8. The recordings show strong non-linearities and the maximum angle deviation approx. in proportion to the travel range.

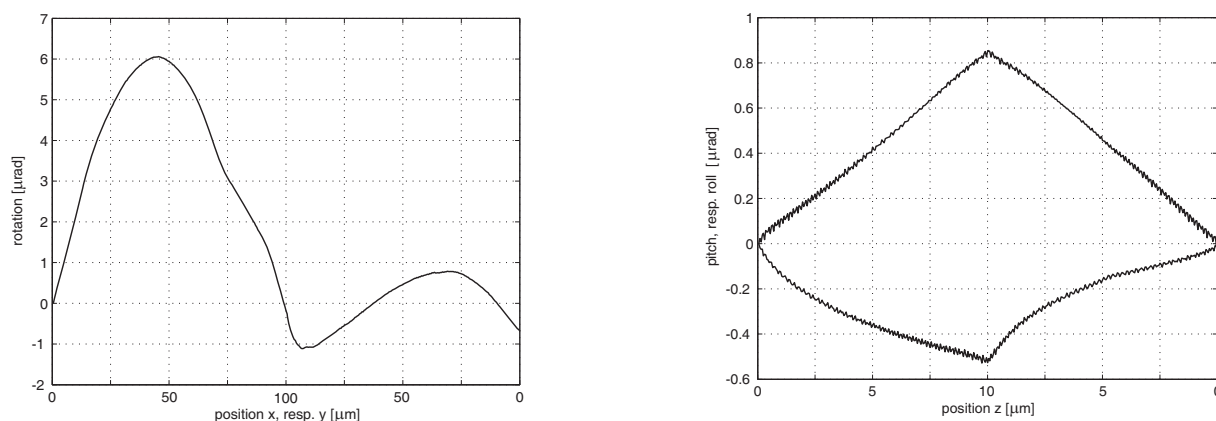


Fig. 8. Recordings of angle deviations. First diagram represents rotation of the stage in the horizontal plane (yaw) during diagonal motion in both x and y axes, the second pitch and roll during vertical motion along z axis.

In the horizontal plane the angle deviation (yaw) was measured during diagonal motion incrementing both x and y position simultaneously with the vertical z position fixed to mid-travel in forward and reverse direction. Pitch and roll angle deviations are in a separate diagram related to the vertical position. The x and y value was again set to mid-range.

The stage was tested again by recording of the difference between the value measured through capacitive sensors and interferometers. In Fig. 9 the deviations are expressed in a greyscale over the whole horizontal plane. The first image represents deviations of the capacitive sensor value from theoretical linear position of the stage that is related to time, the second represents similarly the deviations of the interferometer

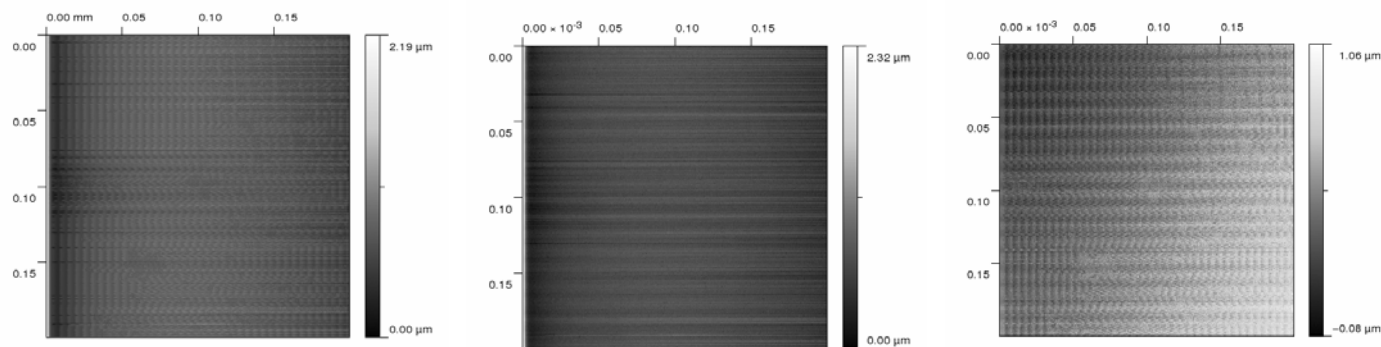


Figure 9: Two-dimensional expression of the differences between the value measured through capacitive sensors and interferometers.

value. The third shows their differences. The differences recording express significant periodicity (modulation) in the horizontal (x) axis which is also clearly visible in the recording of the capacitive sensor output. This periodicity is visible also in Fig. 9, left, bottom curve which indicates it is a systematic error of the capacitive sensor independent on the dynamic effects of the stage positioning. This shows how important improvement in resolution and precision the interferometric displacement monitoring can be.

6. Operation with AFM microscope

The operation of the positioning and measuring system was tested with an AFM (Atomic Force Microscope) head mounted on a tripod upon the frame. A simple AFM scanning head with optical feedback based on laser diode, set of mirrors and quadrant detector was assembled. For fast scanning a small range z-axis piezo was added to the cantilever holder. The signal from four-quadrant detector was processed digitally by single chip microcontroller in order to obtain feedback data used by both table and z-axis piezo in the head. The Z-axis piezo in the head was recalibrated using the scanning table and interferometer before each measurement as a part of sample feedback adjustment.

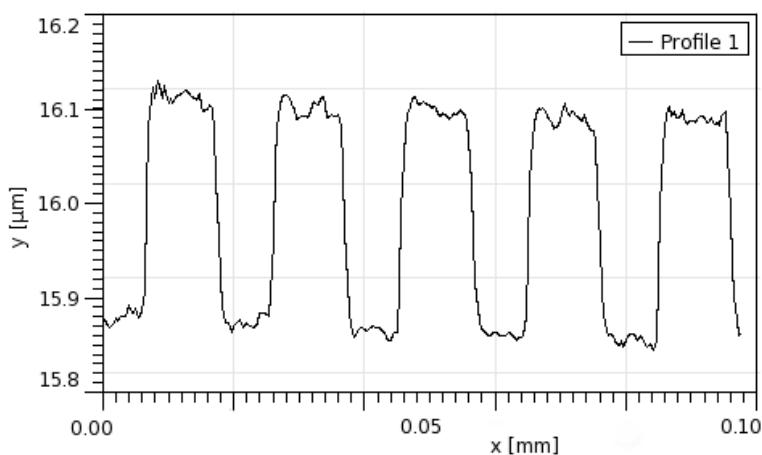
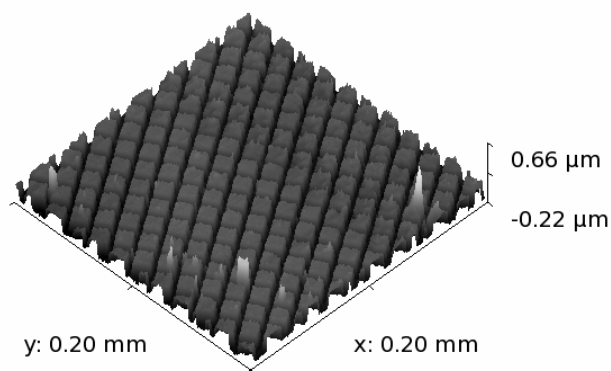


Figure 10: Left: image of a fragment of an etalon of two-dimensional grating; right: an example of a recorded profile achieved by vertical calibrated positioning of the AFM tip.

The whole assembly with AFM microscope was tested by imaging and measuring of an etalon with two-dimensional grating. The image of a fragment of the grating is in figure 10 together with a scanned profile over a small range. Positioning on the horizontal plane is performed with the nanopositioning table while in the vertical axis the PZT of the AFM microscope is used

being previously calibrated through the interferometric measured vertical positioning of the stage.

7. Etalon Calibration

The primary intention of the whole system operation is at the department of nanometrology of the Czech Metrology institute in Brno. The effort that is presented here was at this stage finalized with evaluation of the overall uncertainty by testing on a calibrated etalon of a grating which could be independently verified through diffraction techniques. The overall values are in this stage of development limited primarily by mechanics of the assembly but represent an overview of the performance.

A two-dimensional grating with 2 μm steps was selected. The evaluation of overall uncertainty included verification of the laser wavelength by a calibrated wavemeter and comparison of the grating dimensions derived from measurement via the metrological AFM and through laser diffraction technique. The image of a fraction of the grating is in Figure 11 together with a typical profile in the x-axis.

Evaluation of the grating spacing was done by comparing of the position derived from built-in capacitive sensors and position measured through the interferometric frame.

Laser based diffraction technique allowed measurement of the overall value of the groove spacing with small uncertainty compared to statistical evaluation of average value from AFM measurement. Results are summarized in table 1.

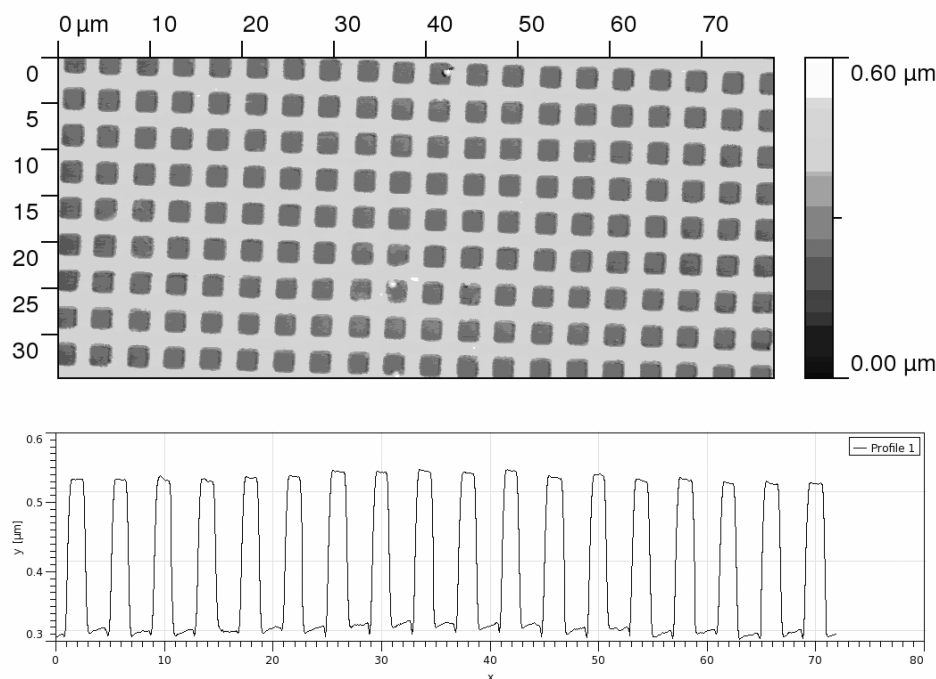


Figure 11: Image of the two-dimensional etalon grating used for calibration and uncertainty evaluation together with a cross-section of the profile

	capacitive sensors	interferometer	diffraction
x-direction	3995 ± 6 nm	4001 ± 6 nm	3996.7 ± 1.8 nm
y-direction	4002 ± 10 nm	4001 ± 10 nm	3994.2 ± 1.1 nm

Table 1: Spacing of the measured grating with estimated statistical uncertainty.

Statistical uncertainty associated with the AFM measurement either through capacitive sensors or interferometers includes angle errors caused by non-linear motion of the stage. Together with uncertainty of the coincidence of the measuring tip and measuring axes of the interferometers this introduces additional errors. Further improvement towards closed-loop operation derived from the interferometers will help significantly. The evaluation of uncertainty was performed with the first version of the system where the correction of the angle errors was not yet operational. It seems that it will represent further improvement.

8. Conclusion

Interferometric system presented here represents a nanometrology tool still under development. Interferometric monitoring and further full feedback servo control of the positioning derived from the interferometer value represents significant improvement for calibration of grating-type etalons through local probe microscopy where the resulting image can be referenced to the interferometer measured position.

First experiments showed that the six-axis interferometric monitoring with a wide base for independent angle evaluation can give information about angle errors with a resolution on the level of few tens of nanoradians. This seems to be an excellent value and a full control of the straightness of motion will be an answer to problems with alignment of the measuring axis and center of the AFM tip. With a positioning of the stage without angle shifts the full traceability can be ensured and it is possible to suppress uncertainty associated with Abbe errors resulting from different motion path of the probe and the interferometer value due to angle tilt.

Overall angle deviations over the whole range of motion did not exceed 10 μ rad. Introduction of small-

range PZT transducers for real-time control (Fig. 8) and closed-loop operation is able to eliminate all the angle deviation errors with additional positioning on several μm level.

Independent adjustment of all collimators feeding the laser light into interferometric units brought a significant improvement of performance where any cosine errors could be also eliminated. An overview of the whole setup is given in the photo in Fig. 12 where the stage and interferometers are visible with removed sample table.

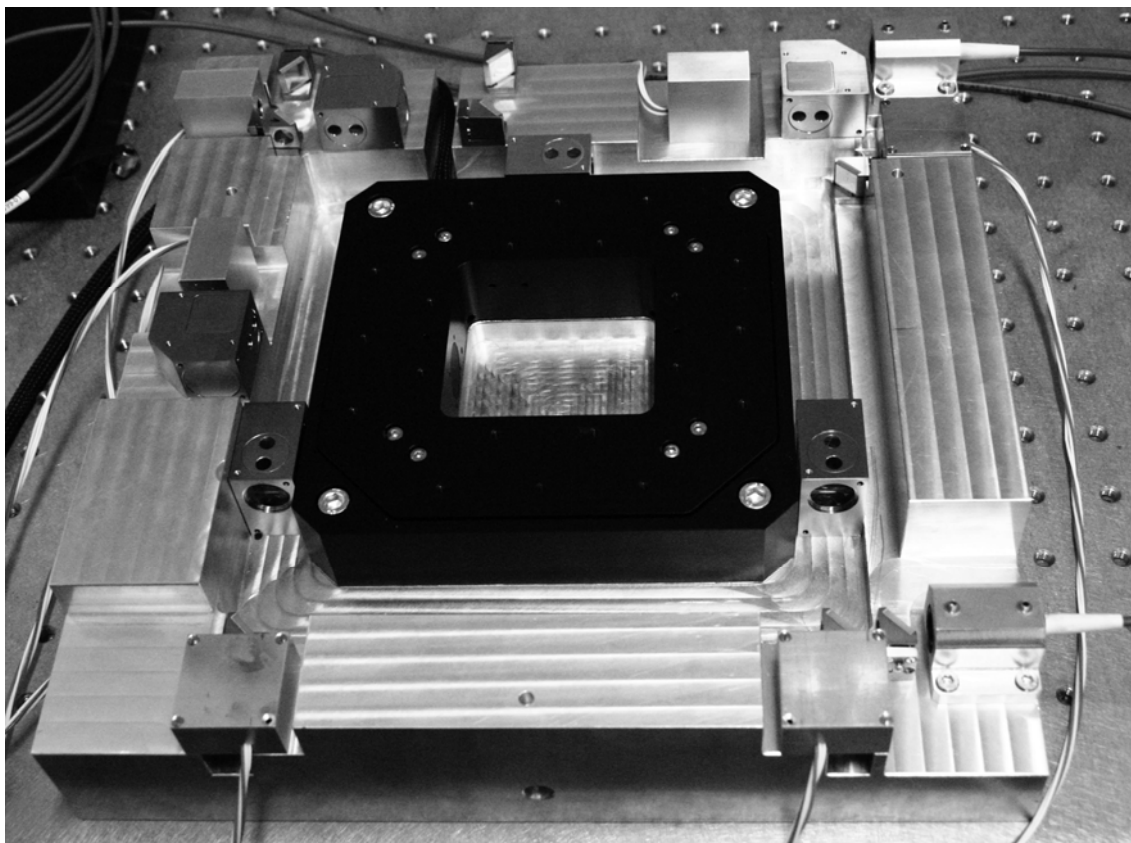


Figure 12: Photo of the first arrangement of the interferometric positioning assembly for AFM based nanometrology.

9. Acknowledgements

The authors wish to express thanks for support to the grant projects from Ministry of Education, Youth and Sports of CR, projects No.: LC06007, the AS CR, project No.: KAN311610701, Ministry of Industry and Commerce, projects No: FR-TI1/241 and GA CR, project: GA102/09/1276.

References:

- [1] Wang, T.-H., Lu, M.-C., Hsu, C.-C., Lu, Y.Y., Image ruler and its applications in distance and area measurement, WSEAS Transactions on Systems, 2007, Vol. 6, No. 5, pp. 901-907.
- [2] Mèndez, J., Parsiani, H., Sanchez, E., Remote sensing of atmospheric particles using LIDAR, Calipso satellite, & AERONET: Algorithm development, WSEAS Transactions on Systems, 2009, Vol. 8, No. 1, pp. 86-95.

- [3] Kumarajah, K., Menon, P.S., Ismail, M., Yeop, B.Y., Shaari, S., MQW design parameter variation in a 1.5 μm wavelength InP-based LW-VCSEL, WSEAS Transactions on Electronics, 2008, Vol. 5, No. 11, pp. 437-446.

- [4] Korpelainen V and Lassila A (2006) Calibration of a commercial AFM: traceability for a coordinate system, Meas. Sci. Technol., 18: 395-403.

- [5] Quinn T J (1992) Mise en pratique of the definition of the metre, Metrologia 1993/94, 30: 523-541.

- [6] Jäger G, Gruenwald R, Manske E, Hausotte T and Fuessl R (2004) A nanopositioning and nanomeasuring

machine: operation—measured results *Nanotechnology and Precision Engineering* 2: 81-4.

[7] Weckenmann A, Hoffmann J and Schuler A (2008) Development of a tunnelling current sensor for a long-range nano-positioning device, *Meas. Sci. Technol.* 19: 064002, 7pp.

[8] Dai G, Pohlenz F, Min Xu, Koenders L, Danzebrink H U and Wilkening G (2006) Accurate and traceable measurement of nano- and microstructures, *Meas. Sci. Technol.*, 17: 545–552.

[9] Otsuka J, Ichikawa S, Masuda T, et al. (2005) Development of a small ultraprecision positioning device with 5 nm resolution, *Meas. Sci. Technol.*, 16: 2186-2192.

[10] Kim J W, Kang C S, Kim J A, et al. (2007) A compact system for simultaneous measurement of linear and angular displacements of nano-stages *Optics Express*, 15: 15759-15766.

[11] Koops K R, van Veghel M G A, Kotte G J W L and Moolman M C (2007) Calibration strategies for scanning probe metrology, *Meas. Sci. Technol.*, 18: 390–394.

[12] Hou W and Wilkening G (1992) Investigation and compensation of the nonlinearity of heterodyne interferometers, *Prec. Eng.* 14: 91-98.

[13] Čip O and Petru F (2000) A scale-linearization method for precise laser interferometry. *Meas. Sci. Technol.*, 11: 133-141.

[14] Petru F and Čip O (1999) Problems regarding linearity of data of a laser interferometer with a single frequency laser. *Precision Engineering*, 23: 39-50.